Facile and fast fabrication of high structure-stable thin film nanocomposite membrane for potential application in solvent resistance nanofiltration

Yongliang Chen[1,2], Milos Toth[2], Chunju He[1]*

[1]State Key Laboratory for Modification of Chemical Fibers and Polymer Materials

College of Materials Science and Engineering

Donghua University

Shanghai, 201620, P.R. China

[2]School of Mathematical and Physical Sciences, University of Technology,

Sydney,P.O. Box 123, Broadway, New South Wales 2007, Australia

Corresponding author：Chunju He; Email: chunjuhe@dhu.edu.cn

Abstract: We propose an interfacial design strategy to prepare novel, highly structure-stable thin film nanocomposite (TFN) nanofiltration (NF) membranes. It employs NMG-assisted dopamine modification on nanoparticles and a substrate, followed by interfacial polymerization. Our approach overcomes two problems that are typical of composite membranes – a weak interlayer interactive force, and poor compatibility between inorganic nanoparticles and a polymer matrix in nanocomposite membranes. The TFN membrane presented here has a high methanol permeance (2.18 $L \cdot m^{-2} \cdot h^{-1} \cdot bar^{-1}$) and a high rejection (99.1%) to acid red 18 (MW=509 $g \cdot mol^{-1}$), which is superior to commercial solvent resistant NF (SRNF) membranes and most literature on SRNF membranes. More importantly, our TFN membranes exhibit a high degree of structural stability, demonstrated by immersion in three organic solvents for 15 days and a two day continuous filtration test. Our strategy is facile and highly flexible, has high potential for deployment in SRNF, and may stimulate the development of practical SRNF applications in the near future.

1. Introduction

Recently, solvent resistant nanofiltration (SRNF) has received extensive attention as an emerging, green purification technique. SRNF is attractive because it is environmentally friendly, energy efficient and inexpensive compared to common solvent purification techniques such as distillation and molecular sieving [1-3]. To date, most SRNF membranes have been made from polyimide, polydimethylsiloxane or polyacrylonitrile, which are typically integrally skinned asymmetric membranes that suffer from solvent permeation limitations [4-6]. To overcome this problem, thin film composite (TFC) membranes comprised of a selective layer and a support layer have been proposed as an alternative, because performance can be optimized by tuning their chemical constituents and the structure of the layer pair [7].

Currently, practical applications of NF membranes are dominated by TFC membranes prepared by interfacial polymerization. However, in general, there is no strong interaction between the selective layer and the substrate in most TFC membranes. This results in partial delamination of the selective layer from the substrate after prolonged immersion in organic media due to differential swelling, leading to a reduction in membrane separation performance [8, 9] which seriously hampers the application of most composite membranes in SRNF. To date, a number of solutions to this problem have been proposed, such as creating covalent, ionic linkage or constructing a middle layer with strong adhesion between the substrate and the active layer [10-13]. These are, however, impractical due to high process complexity.

Based on mussel-inspired chemistry, a simple and facile dopamine (DA) self-polymerization process has been proposed as a solution to the poor interactive force problem by creating a highly adhesive polydopamine (PDA) intermediate or selective layer [8, 14-17]. However, in general, the dopamine deposition process is time-consuming and heterogeneous, which greatly impedes practical applications. To mitigate this, Yan et al [16] adopted a 4 hour polyethyleneimine (PEI)/ DA co-deposition process to prepare a homogeneous PEI/PDA composite NF membrane

with low separation efficiency, i.e. a water flux of 1.7 $L \cdot m^{-2} \cdot h^{-1} \cdot bar^{-1}$. Furthermore, we have previously adopted a 2 hour NMG-assisted deposition process to prepare a novel PDA composite NF membrane with a loose layer, i.e. a sodium sulfate rejection of 81.2% [8]. Both approaches fail in achieving a dopamine-based NF membrane with high flux and high salt rejection, although the deposition time has been greatly diminished. Therefore, it is desirable to explore preparation of dopamine composite membranes with high separation performance as well as a time-saving deposition mode.

Recently, the incorporation of nanoparticles (NPs) into the active layer of TFC membranes (called TFN membranes) has proved to be an effective method to improve flux and/or selectivity [1, 7, 18-22]. However, the poor compatibility between polymers and NPs usually results in the formation of interface voids, thus reducing separation efficiency of composite membranes. Although some reports toward surface modification of inorganic NPs demonstrated its effectiveness at improving the compatibility between inorganic filler and polymer matrix, some issues met by the practice such as uncontrollable chemical process and time-consuming separation technology have seriously impeded their practical use [20, 23-26]. Therefore, it is highly worthwhile to explore facile approaches for solving the interface issue.

In this work, we introduce a facile and fast interfacial design strategy to prepare highly structure-stable TFN NF membranes. It employs a fast NMG-assisted dopamine polymerization process followed by facile interfacial polymerization. Fast dopamine deposition coats the support and NPs with an ultrathin PDA coating that contributes to high structural stability of the TFN membrane and improved compatibility between inorganic nanoparticles and the polymer matrix. Furthermore, the separation layer is formed via interfacial polymerization between active groups in aqueous phase (i.e. the phenol and amine groups of the residual DA and NMG) and acyl chloride groups of TMC in organic phase. The resulting TFN NF membranes show favorable separation performance, exceeding that of previously reported dopamine-based NF membranes. More importantly, the membranes show strong structural stability and excellent separation performance in organic solvents,

indicating a huge potential for SRNF applications.

2. Experiment

2.1 Materials

PES substrate with 10 KDa molecular weight cut off was provided by Risingsun Membrane Technology Co. Ltd. (Beijing, China). N-methyl-Dglucamine (NMG) and Dopamine hydrochloride (DA) were provided by Energy Chemical (Shanghai, China). Trimesoyl chloride (TMC, 98%) was obtained from Sigma-Aldrich. In addition, 2-Amino-2-(hydroxymethyl)-1,3-propanediol (Tris) was obtained from TCI (Shanghai, China). Hexane, methanol (MeOH), ethanol (EtOH), isopropanol (IPA), inorganic salts (Na_2SO_4, NaCl, $MgSO_4$ and $MgCl_2$), rose bengal ($C_{20}H_2Cl_4I_4K_2NaO_5$, Mw = 1073), acid red 18 ($C_{18}H_{13}N_3Na_2O_8S_2$, Mw = 509) and methyl orange ($C_{14}H_{14}N_3NaO_3S$, Mw=327) were purchased from Sinopharm Chemical Reagent Co. Ltd. (Shanghai, China). SiO_2 nanoparticles (30 nm) were purchased from Aladdin (China).

2.2 Membrane preparation

As is shown in Figure 1, the preparation of both DA-NMG/TMC and DA-NMG-Silica/TMC composite membranes was accomplished in two stages. First, NMG and DA were successively dissolved quickly in buffer solution (pH=8.5, 20mM Tris) via ultrasonication. The PES substrate was quickly immersed in the above mixed solution and shook at 25℃ for 2 min via ultrasonication to ensure appropriate NMG-assisted DA self-polymerization and full soaking in the water phase. Then, the substrate was taken out and vertically hung in air for approximately 5 min to remove excess water. Second, the substrate was immersed in a 0.3% TMC hexane solution to induce interfacial polymerization. Finally, the obtained DA-NMG/TMC composite membranes were post-treated at 50℃ for 20 min to promote further interfacial reaction. The preparation of DA-NMG-Silica/TMC composite membranes followed the same procedures as above, except that silica nanoparticles were dispersed in the Tris solution via ultrasonication for 2 h prior to the addition of NMG and DA.

We use the label M-0 to represent the DA-NMG/TMC composite membrane, and M-0.01, M-0.1, M-0.2 and M-1 to represent the DA-NMG- SiO_2/TMC composite membranes, corresponding to SiO_2 NP compositions of 0.01%, 0.1%, 0.2% and 0.1%.

2.3 Membrane characterization

Fourier transform infrared spectrometry (FTIR, Nicolet 8700, USA) and X-ray photoelectron spectroscopy (XPS, Shimadzu AXIS Ultra DLD, Japan) were used to investigate the chemical structure of the selective layers. Specifically, the membranes were tested by FTIR with an attenuated total reflectance accessory and spectra in the range of 4000-400 cm^{-1} were obtained via the accumulated average of 32 scans at 4 cm^{-1} resolution. In addition, the membranes were examined by XPS with a monochromated AL K X-ray source (1486.6 eV) and the spectral were obtained via averages of five scans.

A scanning electron microscope (SEM, Hitachi S-4800, Japan)) was used to characterize the membrane morphology. Specifically, samples were first vacuum freeze-dried, then fractured in liquid nitrogen and finally sputter-coated with Au before testing. Top-down and cross-sectional images were obtained using an accelerating voltage of 5.0 kV.

A streaming potential measurement (DelsaNano, Beckman Coulter, USA) was used to characterize surface zeta potentials of the membranes. Specifically, the membranes were characterized by the nanoparticle size analyser and the surface zeta potentials of the membranes under different pH were obtained by switching to the test mode of zeta potential with 15 V.

Contact angle (CA, OCA40Micro, Germany) was adopted to evaluate the surface hydrophilicity of the membranes. Specifically, CA measurement of the membranes was conducted with 3 μl deionized water dropping on the membrane surface and CA were recorded by averaging five measurements.

2.4 Separation performance of the membranes

The detailed testing process has been described in our previous report [9]. In brief, the separation performance of the membranes was tested using a cross-flow filtration rig with a fixed effective area under 6 bar at 25±2 ℃. Before testing, every membrane was first pre-pressured at 7 bar for about 30 min to obtain steady state permeation. Moreover, the membranes were stored into the testing solvent for 48h prior to the above operation. In addition, 1 $g \cdot L^{-1}$ salt solution and 0.05 $g \cdot L^{-1}$ dye solution were used as initial feed solutions. The dye concentration was detected using a UV-vis spectrophotometer. The salt concentration was measured by electrical conductivity. The test of the membrane separation performance in organic solvents employed the same conditions as in aqueous solutions.

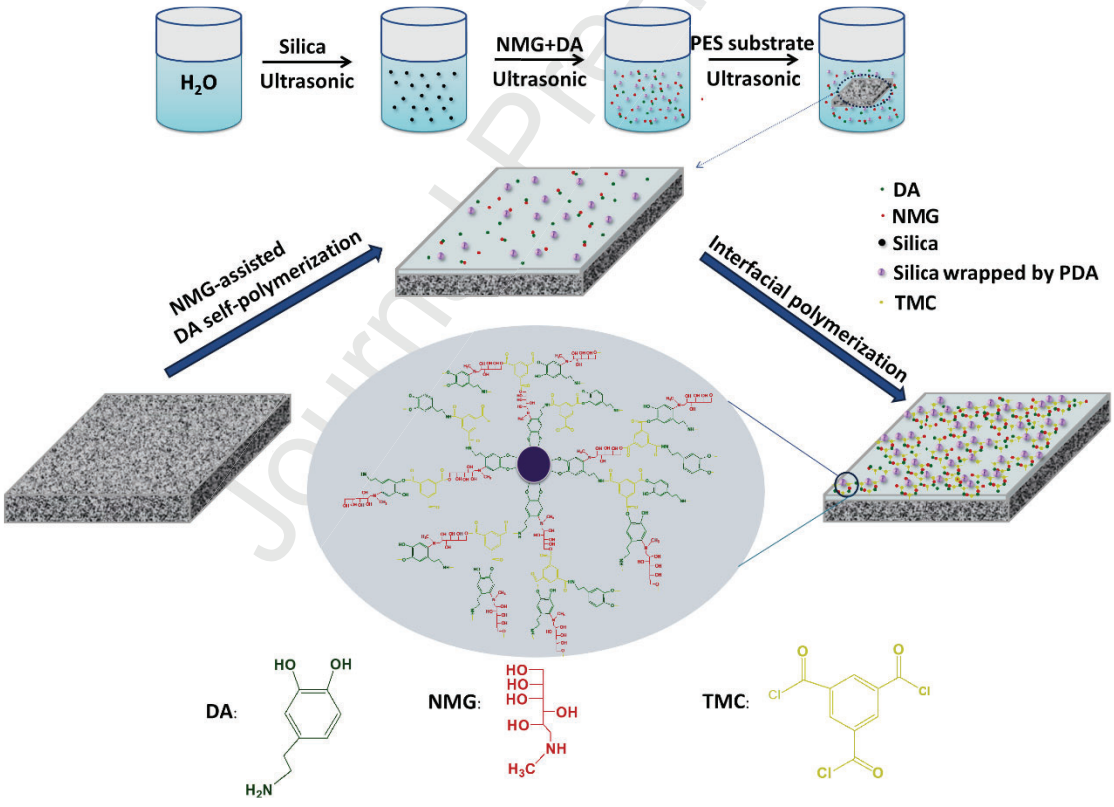

Figure 1. Schematic illustration of the preparation process for the DA-NMG-SiO_2/TMC composite membrane

3. Results and Discussion

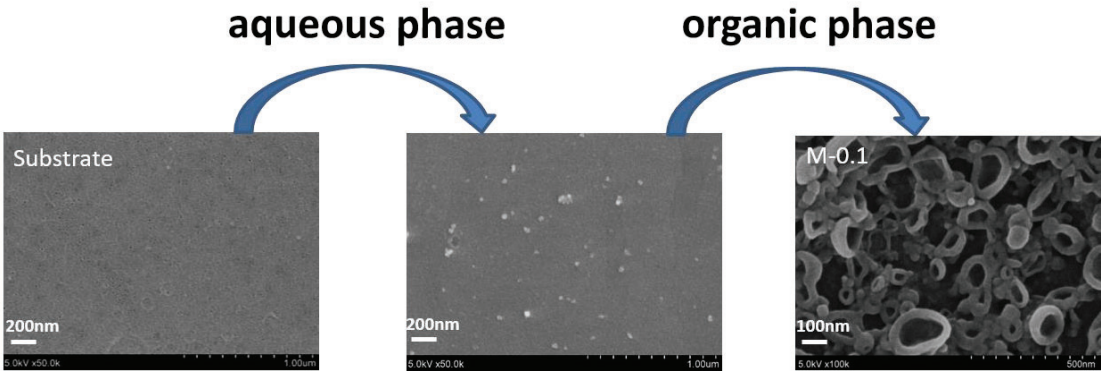

Figure 2. SEM images showing the surface morphology of the substrate before and after immersion in the aqueous solution, and subsequent immersion in the organic solution to form M-0.1

3.1. Formation and characterization of PES-supported dopamine-NMG-SiO_2/TMC nanocomposite membranes

A schematic diagram of the manufacture process of the DA-NMG-SiO_2/TMC nanocomposite membrane is illustrated in Figure 1. Firstly, a PES support is immersed in an aqueous solution containing NMG, DA and SiO_2 NPs for 2 min under ultrasonication. During the process, NMG can facilitate fast polymerization of DA and the homogeneous deposition of PDA, which yields a PES substrate and NPs with an ultra-thin NMG-assisted PDA coating layer [8]. As is shown in Figure 2, after immersion in the aqueous solution, the substrate contains uniformly-dispersed NPs and a reduced pore size, which is ascribed to the formation of a PDA coating layer. Next, the membrane is immersed in an organic solution containing TMC, in order to undergo interfacial polymerization, which yields a typical morphology characteristic of interfacial polymerization (the evenly dispersed nodule surface structure of the resulting M-0.1 as is shown in Figure 2) [27, 28]. It is deduced that the formation of an active layer on the support originates from an interfacial reaction between active groups (including the amine and phenol groups of residual DA, hydroxy groups of NMG and catechol groups of PDA) and acyl chloride groups of TMC, which are characterized below by FTIR and XPS.

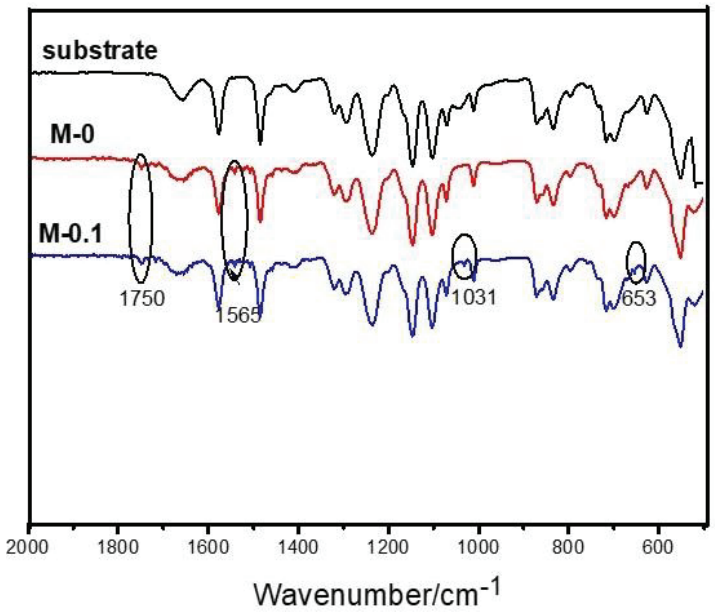

Figure 3. ATR-FTIR spectra of PES substrate, M-0 (NMG-DA/TMC composite membrane) and M-0.1 (NMG-DA-SiO_2/TMC composite membrane)

Chemical composition of the support and the composite membranes was investigated by ATR-FTIR (Figure 3). Compared to the typical bands of the PES support, new peaks are observed in spectra of the composite membrane at 1750 cm^{-1} and 1565 cm^{-1}, corresponding to C=O vibrations from ester bonds, and C=O and C-N vibrations from amide bonds. These indicate the occurrence of interfacial polymerization, resulting in the formation of NMG-DA/TMC layers on the PES support. [29, 30]. In addition, new peaks at 1031 cm^{-1} and 653 cm^{-1} in spectra of the NMG-DA-SiO_2/TMC nanocomposite membrane are assigned to anti-stretching vibration and stretching vibration of Si-O, which indicates the existence of SiO_2 NPs in the NMG-DA/TMC layer.[30]

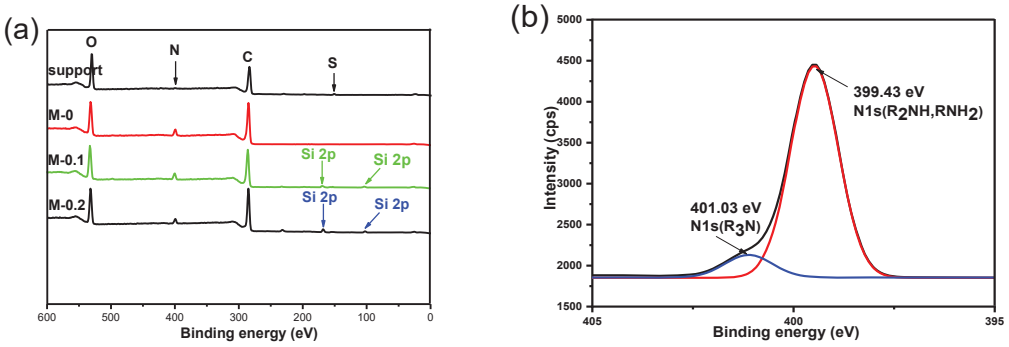

Figure 4. (a) XPS spectra of the PES support, M-0, M-0.1 and M-0.2, (b) N 1 s spectra of M-0. Note: the high resolution N 1s spectra of M-0.1 and M-0.2 show the same spectra as M-0. For clarity, the fits are shown only for M-0

Chemical composition of the membranes is further analyzed by XPS. As is shown in Figure 4a, M-0 is characterized by a nitrogen and a sulfur peak that is present and absent, respectively, in XPS spectra of the PES support, indicating that the substrate is fully covered by the active layer. The silicon peak appears in M-0.1 and M-0.2, proving the existence of silica in the selective layer of the nanocomposite membranes. In addition, as is shown in Figure 4b, a high-resolution XPS spectrum of the N peak in M-0 indicates the existence of R_3N deriving from the nitrogen in NMG. This indicates that NMG participates in the process of interfacial polymerization, which also proves the development of a DA-NMG/TMC layer instead of the formation of a DA/TMC layer on the PES substrate. In addition, Table 1 compares the O/N ratios of active layers with different silica concentrations. As the SiO_2 NPs concentration is increased from 0 to 0.2%, the O/N ratio of the resulting membranes is increased, indicating the inhibition of interfacial polymerization by the added SiO_2 NPs, which may result in a change in the degree of cross-linking of the active layer, consistent with some reports [30-33].

Table 1. Surface chemical compositions of the PES support and the resulting membranes from XPS (in atomic percent)

sample	C	O	N	S	Si	O/N
PES substrate	69.46	26.19	-	4.35	-	-
M-0	69.97	22.28	7.75	-	-	2.87
M-0.01	70.02	22.44	6.89	-	0.65	3.26
M-0.1	67.2	23.62	7.21	-	1.96	3.28
M-0.2	69.18	23.55	5.01	-	2.26	4.7

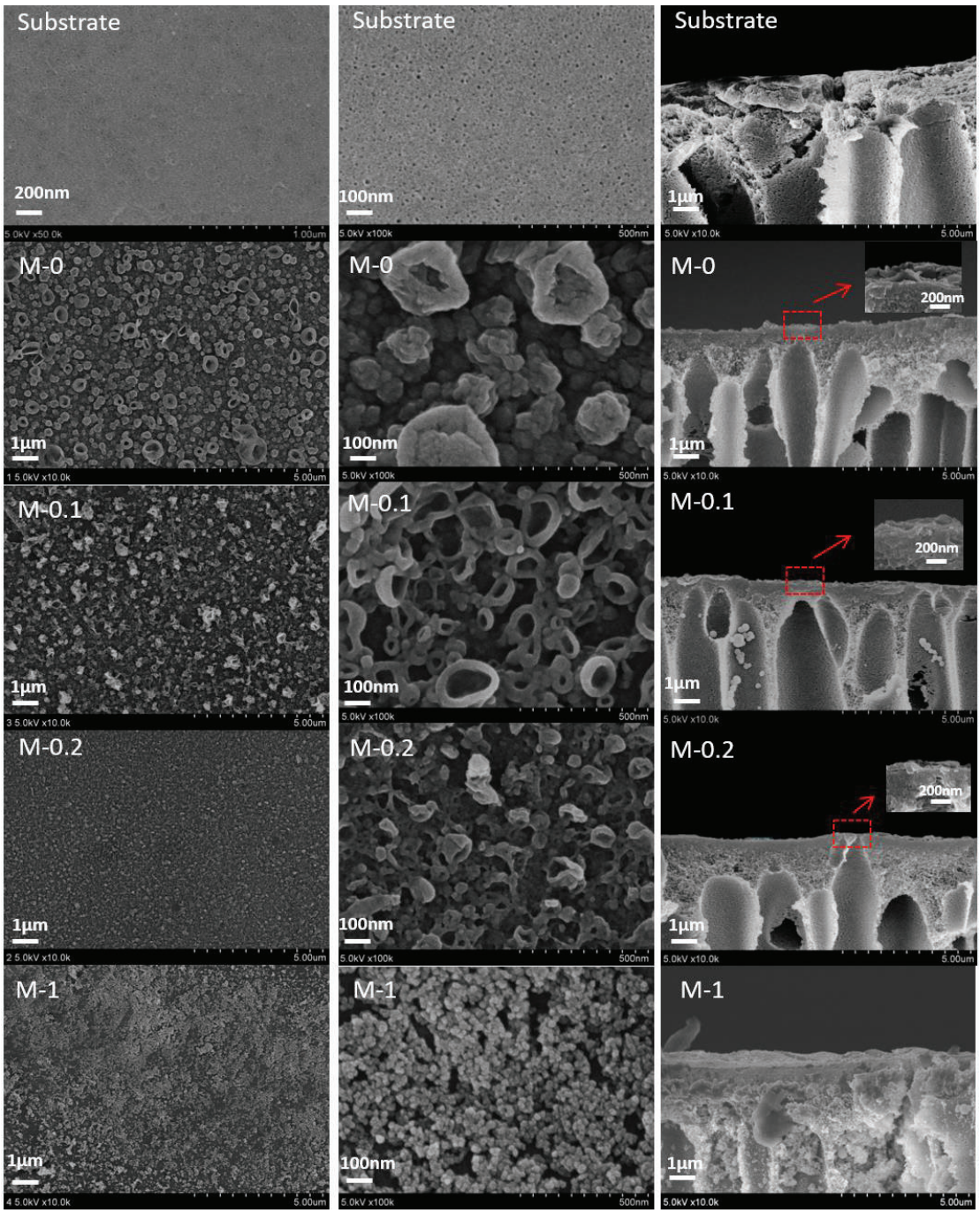

Figure 5. Low magnification surface SEM images (left), high magnification surface SEM images (middle) and cross-sectional images (right, the insets shows high-magnification extracts of the cross-sectional images) of the substrate, M-0, M-0.1, M-0.2 and M-1

The surface morphologies of the membranes are shown in Figure 5 (left and middle). Compared to the substrate, M-0 has a rough surface packed by the evenly-dispersed nodule structure, which is typical of interfacial polymerization [27,

28]. Such a nodule structure has been reported to result from seeds that form in a preliminary stage of interfacial polymerization and subsequently attract additional monomers, the concentration of which determines the size of the nodules [28, 34, 35]. As SiO_2 NPs are inserted into the selective layer of the membrane, a relatively smooth surface morphology (M-0.1 and M-0.2) with a smaller size of the nodular structure is obtained. It is reasonable to deduce that the SiO_2 NPs may inhibit the diffusion of DA, resulting from adsorption and steric hindrance of NPs, thereby reducing the regional monomer concentration near the seeds and ultimately resulting in the formation of smaller nodule structures. When the SiO_2 NP concentration is further increased to 1wt%, the steric hindrance effect greatly impedes the interfacial polymerization process, thereby giving rise to a uniform and ordered layer without a nodule structure (M-1). Moreover, the ordered nanoscale surface with reduced silica nanoparticle aggregation observed in M-1 (which has an ultrahigh SiO_2 NPs concentration) also suggests that the SiO_2 NPs have been dispersed uniformly in the selective layer of M-0.1 and M-0.2 (which have lower SiO_2 NPs concentrations).

Furthermore, the cross-sectional morphologies of the membranes in Figure 5 (right) show that a thin selective layer formed on the support of M-0, M-0.1 and M-0.2. The selective layers of M-0 and M-0.1 are each approximately 200 nm thick, but the thickness of the selective layer for M-0.2 is approximately 160 nm. The reduced thickness is caused by the stronger steric hindrance effect of high loading of SiO_2 NPs, which reduces the diffusion of monomers in the aqueous solution during the process of interfacial polymerization [34].

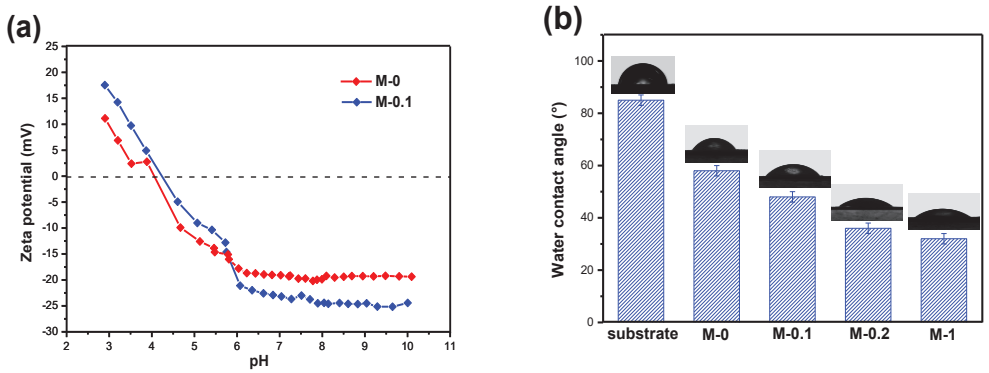

Figure 6. (a) Zeta potential of M-0 and M-0.1 at various pH values, (b) Water contact angle of the substrate, M-0, M-0.1, M-0.2 and M-1

During the water treatment, membrane surface charge is a key factor for attaining high rejection to charged solute. Figure 6a shows the zeta potentials of M-0 and M-0.1 at various pH values. In general, the NF process is conducted at a pH of approximately 6.0, thus both M-0 and M-0.1 are negatively charged, which is ascribed to charged carboxyl groups resulting from the hydrolysis of unreacted acyl chloride groups [32, 36, 37]. In addition, M-0.1 has a higher negative surface charge than M-0, since the embedded NPs reduce the diffusion of dopamine, resulting in development of the active layer with more unreacted acyl chloride groups. The higher surface negative charge will result in a higher rejection to negatively charged solutes because of the Donnan and dielectric effects [8, 38].

Improved surface hydrophilicity can facilitate higher affinity of a membrane surface to water, which contributes to an improvement in membrane separation performance. As is shown in Figure 6(b), the WCA value of M-0 is decreased to 58° compared to the PES support, indicating better wetting properties, which is ascribed to the unreactive hydroxyl groups and carboxylic acid functional groups generated by the hydrolysis of unreactive acyl chloride [31]. Furthermore, impregnation of SiO_2 NPs into the selective layer continues to decrease the WCA value of the resulting membranes, indicating that surface hydrophilicity is further improved.

3.2 Separation performance of the resulting membranes in water treatment

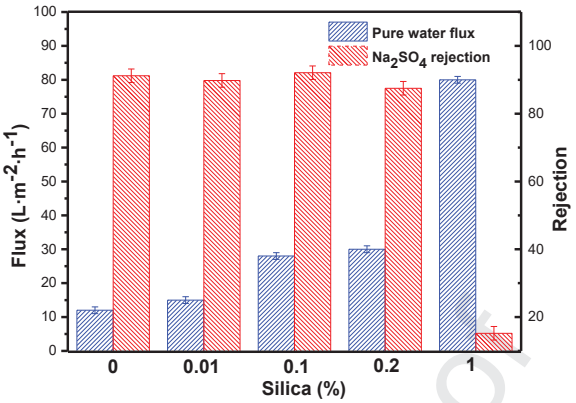

Figure 7. Effect of SiO_2 NP loading on the separation performance of the NMG-DA-SiO_2/TMC nanocomposite membranes

Figure 7 shows the effect of SiO_2 NP loading on the separation performance of the membranes. As the SiO_2 NP loading is increased from 0 to 0.2%, pure water flux is increased from 12 $L \cdot m^{-2} \cdot h^{-1}$ to 30 $L \cdot m^{-2} \cdot h^{-1}$ while Na_2SO_4 rejection of the resulting membranes doesn't significantly change, which is ascribed to the improvement of membrane surface hydrophilicity and the formation of assembled interfacial paths between SiO_2 NPs and polymer interface [20]. In addition, when SiO_2 NP loading is further increased to 1%, M-1 shows the worst separation performance, which is ascribed to the formation of a discontinuous skin layer (seen in Figure 5 (M-1)) caused by significant interference of interfacial polymerization by excessive SiO_2 NPs.

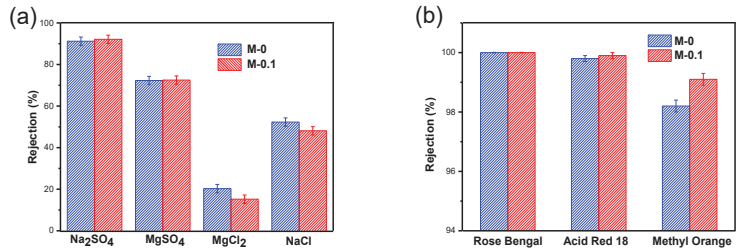

Figure 8. The separation performance of M-0 and M-0.1 for different organic dyes (a) and different inorganic salts (b)

As is shown in Figure 8, different inorganic salts and organic dyes are chosen to further test membrane separation performance. It is well known that the sieving efficiency of charged solutes during an NF process is affected by the steric and Donnan effects [8, 38]. The salt rejections of M-0 and M-0.1 both follow the order Na_2SO_4 > $MgSO_4$> NaCl >$MgCl_2$, in accordance with the salt rejection sequence of a typical negatively charged NF membrane, which is mainly ascribed to Donnan effects [39]. M-0 and M-0.1 both exhibit high rejections to Rose Bengal (1073 Da), Acid Red 18 (509 Da) and Methyl Orange (327 Da), indicating their excellent sieving ability for organic dyes (300 Da–1000 Da). In addition, M-0.1 shows lower rejection to $MgCl_2$ and NaCl than M-0, resulting from formation of the assembled interfacial paths between NPs and polymer matrix, which can allow the penetration of Cl^- ions, thus leading to higher $MgCl_2$ and NaCl permeation [40]. According to Donnan effect, multivalent ions with more positive charge (Mg^{2+}) are easier to pass through the negatively charged membrane than monovalent ions with one positive charge (Na^+), so M-0.1 with positive charge shows lower rejection to $MgCl_2$ than NaCl. However, in comparison to M-0, M-0.1 exhibits higher rejection to organic dyes, $MgSO_4$ and Na_2SO_4,which may be due to a more negatively charged surface of M-0.1 (as is shown in Figure 6(a)), and bigger hydrated ion radius of $SO4^{2-}$ and three dyes that are not small enough to penetrate across the assembled interfacial paths [35]. Furthermore, Table 2 compares the NF performances of the reported composite membranes with dopamine-based selective layer and it can be found that the membranes in this work

exhibit comparable water flux and high rejection to bivalent anions. Overall, the excellent observed separation performance makes the membranes promising for water purification.

Table 2 Comparison of the separation performance between M-0.1 and the reported composite membranes with dopamine-based separation layer

A dopamine-based selective layer	Zeta potential (mv)	Rejection molecule	Rejection (%)	water flux ($L \cdot m^{-2} \cdot h^{-1} \cdot bar^{-1}$)	Ref.
PDA/PEI layer via self-polymerization and PEI grafting	12.1	$MgCl_2$	73.7%	7.2	14
PDA layer via double self-polymerization	5.5	$CaCl_2$	68.7%	11.7	15
PDA/PEI layer via self-polymerization and GA cross-lining	6.5	$MgCl_2$	92.0%	1.7	16
PDA layer via NMG-assisted self-polymerization and GA cross-ling	-4.5	Na_2SO_4	81.2%	10.29	8
PDA/PEI layer via self-polymerization and polymer grafting	-9.5	Na_2SO_4	96.2%	3.3	39
DA-NMG-SiO_2/TMC layer via NMG-assisted self-polymerization and interfacial polymerization (M-0.1)	-14.1	Na_2SO_4	92.1%	4.72	This work

3.3 Structure stability of the composite membranes in organic solvents

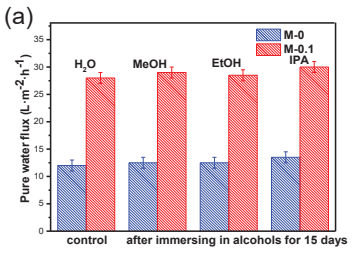

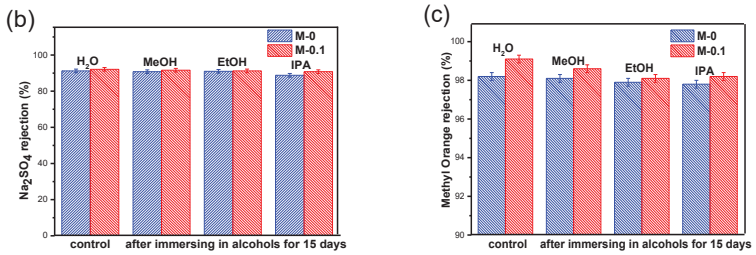

Figure 9. The pure water flux (a), Na_2SO_4 rejection (b) and methyl orange rejection (c) of M-0 and M-0.1 after immersing in organic solvents for 15 days

In common composite membranes, the selective layer may be detached from the PES substrate in organic solvents due to big swelling differences between them, leading to serious deterioration of separation performance. According to some reports, the pure water flux can be increased above 30% for the mostly common PES supported composite NF membrane and the rejection to Na_2SO_4 can be nearly decreased by half after immersing in organic solvents for 1 day [8, 9]. Therefore, the structure stability of as-prepared composite membranes in organic solvents is crucial for applications in SRNF. As is shown in Figure 9a, the pure water fluxes of M-0 and M-0.1 both exhibit no significant change after immersion in organic solvents for 15 days. Furthermore, the rejections to sodium sulfate and methyl orange both decrease slightly, as is shown in Figure 9(b-c). These encouraging results prove that the PES-supported dopamine-NMG/TMC (M-0) and dopamine-NMG- SiO_2 /TMC (M-0.1) composite membranes both show excellent structure stability in organic solvents, due to multiple binding forces of the catechol structure and the crosslink network between the dopamine-based selective layer and PES substrate, which indicates that M-0 and M-0.1 membranes are promising for practical applications in SRNF [8, 41-43].

3.4 Separation performance of the composite membranes in organic solvents

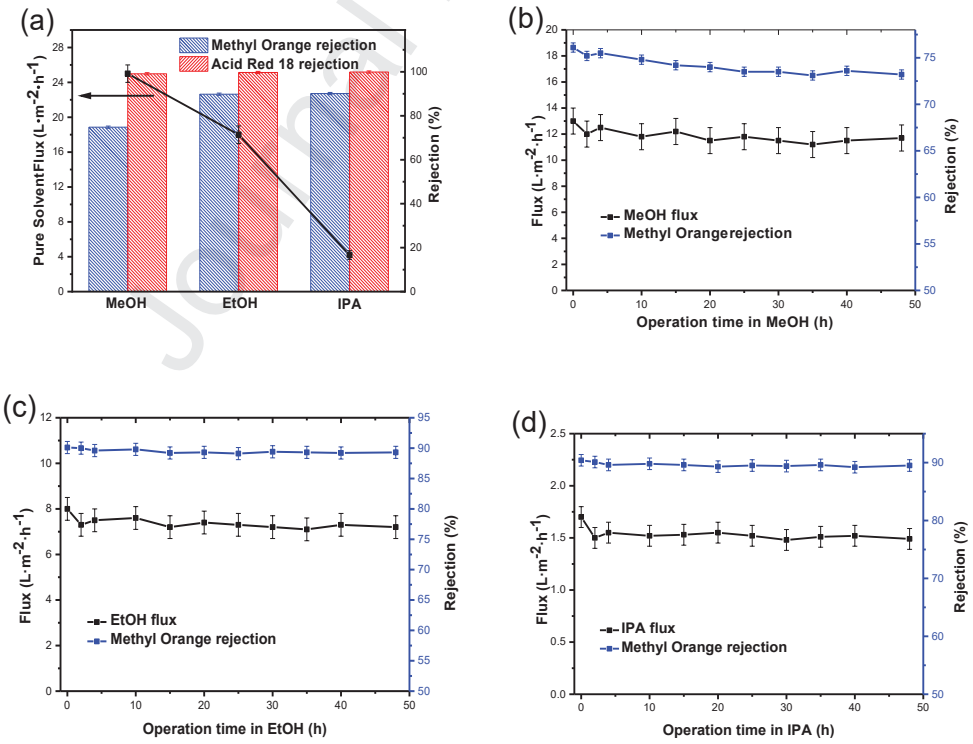

Figure 10. Separation performances of the dopamine-NMG-silica/TMC (M-0.1) composite membrane in various organic solvents; (b-d) long-term performance in various organic solvents

As is shown in Figure 10a, M-0.1 exhibits excellent separation performance in typical organic solvents such as methanol (MeOH), ethanol (EtOH) and isopropanol (IPA), due to the structure stability in solvents and the cross-linked structure of hybrid selective layer. It has been reported that SRNF membranes have a complex transportation mechanism, which is usually controlled by solvent properties (viscosity, surface tension and so on) and mutual interactions among solvent, solute and membrane [1, 44, 45]. Therefore, the pure solvent flux follows the sequence (MeOH > EtOH > IPA), consistent with that of their molar volume and viscosity. However, the dye rejections in alcohols exhibit the opposite trend, which is ascribed to the "dragging effect" of solvent and mutual interactions between solvent and solute [46].

Furthermore, in order to further evaluate feasibility of practical applications in organic solvents, long term performance of M-0.1 is tested using methyl orange and organic solvents (MeOH, EtOH and IPA) as solute and feed solvents, respectively. As is shown in Figure 10(b-d), there are no obvious changes for the separation performance of M-0.1 during two days continuous filtration process, which further proves the strong structural stability of M-0.1 in these solvents.

As is shown in Table 3, M-0.1 has a high size sieving ability, maintaining a comparable solvent flux to (PA/MOFs)/PI membranes containing MIL-53 or ZIF-8 [47] and (PA/SiO_2)/PAN membrane [48], whereas (PA/WCNTs)/PES membranes [49] seem to show the best solvent permeance. In addition, the separation performance of M-0.1 in this study is also superior to that of commercial SRNF membranes (Desal-5-DK, MPF-44 and MPF-50 membranes) [50]. More importantly, it should be possible to prepare novel dopamine nanocomposite membranes containing other NPs such as MOFs and WCNTs via the facile and flexible approach described here, due to universality and versatility of dopamine in membrane fabrication and modification. Such membranes will likely further improve the solvent permeation of the nanocomposite membrane without compromise of retention towards organic dyes, derived from the porosity of MOFs [47], the inner cores of CNTs [51] and so on. These encouraging results indicate that the novel dopamine

nanocomposite membranes provide a promising path for accelerating the deployment of SRNF membranes in practical applications.

Table 3 Comparison of the separation performance among M-0.1, the reported SRNF nanocomposite membranes and commercial SRNF membranes

Membrane material	Nanoparticles	Solvent	Pure Solvent Flux ($L \cdot m^{-2} \cdot h^{-1} \cdot bar^{-1}$)	Solute	Rejection (MW)	Ref.
(PA/MOFs)/PI	MIL-53	MeOH	2.3	Polystyrenes	99% (1000 $g \cdot mol^{-1}$)	47
	ZIF-8	MeOH	2.5	Polystyrenes	99% (1000 $g \cdot mol^{-1}$)	
	MIL-101	MeOH	4.2	Polystyrenes	99% (1000 $g \cdot mol^{-1}$)	
(PA/WCNTs)/PES	SWCNTs	MeOH	7.39	Brilliant blue R	89% (826 $g \cdot mol^{-1}$)	49
(PA/SiO_2)/PAN	SiO_2	IPA	1.45	PEG	99% (1000 $g \cdot mol^{-1}$)	48
Desal-5-DK	-	MeOH	0.5	Erythrosine B	99% (880 $g \cdot mol^{-1}$)	50
MPF-44	-	MeOH	1.88	Erythrosine B	93% (880 $g \cdot mol^{-1}$)	50
MPF-50	-	MeOH	2.5	Erythrosine B	97% (880 $g \cdot mol^{-1}$)	50
M-0.1	SiO_2	MeOH	2.18	Acid Red 18	99.1% (509 $g \cdot mol^{-1}$)	This
				Methyl Orange	78.6% (327 $g \cdot mol^{-1}$)	work
		IPA	0.31	Acid Red 18	99.9% (509 $g \cdot mol^{-1}$)	

	Methyl Orange	92.8% (327 g·mol^{-1})

4. Conclusions

A facile and fast interface design strategy, including fast NMG-assisted DA self-polymerization followed by interfacial polymerization, was introduced in this work to solve the problems of poor structure stability of composite membranes and poor compatibility between NPs and a polymer matrix. The optimized nanocomposite membrane showed a flux increase of over 200% with similar rejection due to the incorporation of SiO_2 NPs, high rejection of bivalent salts and high rejection of organic dyes (300 Da–1000 Da) during water treatment. More importantly, the membranes showed excellent structure stability and separation performance in organic solvents, as well as stability tested by a two-day-long test in organic solvents, which indicates that the PES-supported dopamine-SiO_2 nanocomposite membrane is a very promising candidate for practical applications in SRNF. Moreover, our work paves the way to structure-stable TFN NF membranes that contain different NPs due to the universality and versatility of dopamine in membrane fabrication and modification, and is expected to promote use of SRNF membranes in practical applications.

Acknowledgments

This work is supported by CSC scholarship, grants from the National Science Foundation of China (No.51873034), Program of Introducing Talents of Discipline to Universities (No.111-2-04).

[1] Y.C. Xu, Y.P. Tang, L.F. Liu, Z.H. Guo, L. Shao, Nanocomposite organic solvent nanofiltration membranes by a highly-efficient mussel-inspired co-deposition strategy, Journal of Membrane Science, 526 (2017) 32-42.

[2] S.J. Schneiderman, R.N. Gurram, T.J. Menkhaus, P.C. Gilcrease, Comparative technoeconomic analysis of a softwood ethanol process featuring posthydrolysis sugars concentration operations and continuous fermentation with cell recycle, Biotechnol. Prog., 31 (2015) 946-956.

[3] G. Szekely, M. Gil, B. Sellergren, W. Heggie, F.C. Ferreira, Environmental and economic analysis for selection and engineering sustainable API degenotoxification processes, Green Chem., 15 (2013) 210-225.

[4] X.Q. Cheng, K. Konstas, C.M. Doherty, C.D. Wood, X. Mulet, Z.L. Xie, D. Ng, M.R. Hill, L. Shao, C.H. Lau, Hyper-Cross-Linked Additives that Impede Aging and Enhance Permeability in Thin Polyacetylene Films for Organic Solvent Nanofiltration, ACS Appl. Mater. Interfaces, 9 (2017) 14401-14408.

[5] S. Darvishmanesh, J.C. Jansen, F. Tasselli, E. Tocci, P. Luis, J. Degreve, E. Drioli, B. Van der Bruggen, Novel polyphenylsulfone membrane for potential use in solvent nanofiltration, J. Membr. Sci., 379 (2011) 60-68.

[6] M.F. Jimenez Solomon, Y. Bhole, A.G. Livingston, High flux hydrophobic membranes for organic solvent nanofiltration (OSN)—Interfacial polymerization, surface modification and solvent activation, J. Membr. Sci., 434 (2013) 193-203.

[7] S. Hermans, H. Marien, C. Van Goethem, I.F.J. Vankelecom, Recent developments in thin film (nano)composite membranes for solvent resistant nanofiltration, Curr. Opin. Chem. Eng., 8 (2015) 45-54.

[8] Y.L. Chen, C.J. He, High salt permeation nanofiltration membranes based on NMG-assisted polydopamine coating for dye/salt fractionation, Desalination, 413 (2017) 29-39.

[9] Y.F. Li, Y.L. Su, J.Y. Li, X.T. Zhao, R.N. Zhang, X.C. Fan, J.N. Zhu, Y.Y. Ma, Y. Liu, Z.Y. Jiang, Preparation of thin film composite nanofiltration membrane with improved structural stability through the mediation

of polydopamine, Journal of Membrane Science, 476 (2015) 10-19.
[10] H. Il Kim, S.S. Kim, Plasma treatment of polypropylene and polysulfone supports for thin film composite reverse osmosis membrane, J. Membr. Sci., 286 (2006) 193-201.
[11] H.Y. Deng, Y.Y. Xu, Q.C. Chen, X.Z. Wei, B.K. Zhu, High flux positively charged nanofiltration membranes prepared by UV-initiated graft polymerization of methacrylatoethyl trimethyl ammonium chloride (DMC) onto polysulfone membranes, J. Membr. Sci., 366 (2011) 363-372.
[12] R. Bernstein, E. Anton, M. Ulbricht, UV-Photo Graft Functionalization of Polyethersulfone Membrane with Strong Polyelectrolyte Hydrogel and Its Application for Nanofiltration, Acs Applied Materials & Interfaces, 4 (2012) 3438-3446.
[13] J.M. Peng, Y.L. Su, W.J. Chen, X.T. Zhao, Z.Y. Jiang, Y.A. Dong, Y. Zhang, J.Z. Liu, X.Z. Cao, Polyamide nanofiltration membrane with high separation performance prepared by EDC/NHS mediated interfacial polymerization, Journal of Membrane Science, 427 (2013) 92-100.
[14] R.N. Zhang, Y.L. Su, X.T. Zhao, Y.F. Li, J.J. Zhao, Z.Y. Jiang, A novel positively charged composite nanofiltration membrane prepared by bio-inspired adhesion of polydopamine and surface grafting of poly(ethylene imine), Journal of Membrane Science, 470 (2014) 9-17.
[15] X.L. Li, L.P. Zhu, J.H. Jiang, Z.A. Yi, B.K. Zhu, Y.Y. Xu, Hydrophilic nanofiltration membranes with self-polymerized and strongly-adhered polydopamine as separating layer, Chin. J. Polym. Sci., 30 (2012) 152-163.
[16] Y. Lv, H.C. Yang, H.Q. Liang, L.S. Wan, Z.K. Xu, Nanofiltration membranes via co-deposition of polydopamine/polyethylenimine followed by cross-linking, Journal of Membrane Science, 476 (2015) 50-58.
[17] Y. Xu, Z. Li, K. Su, T. Fan, L. Cao, Mussel-inspired modification of PPS membrane to separate and remove the dyes from the wastewater, Chemical Engineering Journal, 341 (2018) 371-382.
[18] N.A.A. Sani, W.J. Lau, A.F. Ismail, Polyphenylsulfone-based solvent resistant nanofiltration (SRNF) membrane incorporated with copper-1,3,5-benzenetricarboxylate (Cu-BTC) nanoparticles for methanol separation, RSC Adv., 5 (2015) 13000-13010.
[19] L. Shao, X.Q. Cheng, Z.X. Wang, J. Ma, Z.H. Guo, Tuning the performance of polypyrrole-based solvent-resistant composite nanofiltration membranes by optimizing polymerization conditions and incorporating graphene oxide, J. Membr. Sci., 452 (2014) 82-89.
[20] M. Peyravi, M. Jahanshahi, A. Rahimpour, A. Javadi, S. Hajavi, Novel thin film nanocomposite membranes incorporated with functionalized TiO2 nanoparticles for organic solvent nanofiltration, Chemical Engineering Journal, 241 (2014) 155-166.
[21] H. Siddique, E. Rundquist, Y. Bhole, L.G. Peeva, A.G. Livingston, Mixed matrix membranes for organic solvent nanofiltration, J. Membr. Sci., 452 (2014) 354-366.
[22] I. Soroko, A. Livingston, Impact of TiO2 nanoparticles on morphology and performance of crosslinked polyimide organic solvent nanofiltration (OSN) membranes, J. Membr. Sci., 343 (2009) 189-198.
[23] B. Rajaeian, A. Rahimpour, M.O. Tade, S.M. Liu, Fabrication and characterization of polyamide thin film nanocomposite (TFN) nanofiltration membrane impregnated with TiO2 nanoparticles, Desalination, 313 (2013) 176-188.
[24] E.S. Kim, G. Hwang, M.G. El-Din, Y. Liu, Development of nanosilver and multi-walled carbon nanotubes thin-film nanocomposite membrane for enhanced water treatment, J. Membr. Sci., 394 (2012) 37-48.
[25] J. Yin, E.S. Kim, J. Yang, B.L. Deng, Fabrication of a novel thin-film nanocomposite (TFN)

membrane containing MCM-41 silica nanoparticles (NPs) for water purification, J. Membr. Sci., 423 (2012) 238-246.

[26] H. Zhang, H. Mao, J. Wang, R. Ding, Z. Du, J. Liu, S. Cao, Mineralization-inspired preparation of composite membranes with polyethyleneimine-nanoparticle hybrid active layer for solvent resistant nanofiltration, J. Membr. Sci., 470 (2014) 70-79.

[27] M. Safarpour, A. Khataee, V. Vatanpour, Thin film nanocomposite reverse osmosis membrane modified by reduced graphene oxide/TiO2 with improved desalination performance, J. Membr. Sci., 489 (2015) 43-54.

[28] J. Wang, Y.M. Wang, Y.T. Zhang, A. Uliana, J.Y. Zhu, J.D. Liu, B. Van der Bruggen, Zeolitic Imidazolate Framework/Graphene Oxide Hybrid Nanosheets Functionalized Thin Film Nanocomposite Membrane for Enhanced Antimicrobial Performance, ACS Appl. Mater. Interfaces, 8 (2016) 25508-25519.

[29] H. Lee, S.M. Dellatore, W.M. Miller, P.B. Messersmith, Mussel-inspired surface chemistry for multifunctional coatings, Science, 318 (2007) 426-430.

[30] D. Hu, Z.L. Xu, C. Chen, Polypiperazine-amide nanofiltration membrane containing silica nanoparticles prepared by interfacial polymerization, Desalination, 301 (2012) 75-81.

[31] J.-J. Wang, H.-C. Yang, M.-B. Wu, X. Zhang, Z.-K. Xu, Nanofiltration membranes with cellulose nanocrystals as an interlayer for unprecedented performance, Journal of Materials Chemistry A, 5 (2017) 16289-16295.

[32] S.J. Park, W.G. Ahn, W. Choi, S.H. Park, J.S. Lee, H.W. Jung, J.H. Lee, A facile and scalable fabrication method for thin film composite reverse osmosis membranes: dual-layer slot coating, Journal of Materials Chemistry A, 5 (2017) 6648-6655.

[33] H.S. Lee, S.J. Im, J.H. Kim, H.J. Kim, J.P. Kim, B.R. Min, Polyamide thin-film nanofiltration membranes containing TiO2 nanoparticles, Desalination, 219 (2008) 48-56.

[34] X.J. Song, Q.Z. Zhou, T. Zhang, H.B. Xu, Z.N. Wang, Pressure-assisted preparation of graphene oxide quantum dot-incorporated reverse osmosis membranes: antifouling and chlorine resistance potentials, Journal of Materials Chemistry A, 4 (2016) 16896-16905.

[35] J.Y. Zhu, L.J. Qin, A. Uliana, J.W. Hou, J. Wang, Y.T. Zhang, X. Li, S.S. Yuan, J. Li, M.M. Tian, J.Y. Lin, B. Van der Bruggen, Elevated Performance of Thin Film Nanocomposite Membranes Enabled by Modified Hydrophilic MOFs for Nanofiltration, ACS Appl. Mater. Interfaces, 9 (2017) 1975-1986.

[36] A. Soroush, J. Barzin, M. Barikani, M. Fathizadeh, Interfacially polymerized polyamide thin film composite membranes: Preparation, characterization and performance evaluation, Desalination, 287 (2012) 310-316.

[37] C.C. Wamser, M.I. Gilbert, DETECTION OF SURFACE FUNCTIONAL-GROUP ASYMMETRY IN INTERFACIALLY-POLYMERIZED FILMS BY CONTACT-ANGLE TITRATIONS, Langmuir, 8 (1992) 1608-1614.

[38] X.L. Wang, T. Tsuru, S. Nakao, S. Kimura, The electrostatic and steric-hindrance model for the transport of charged solutes through nanofiltration membranes, J. Membr. Sci., 135 (1997) 19-32.

[39] L.X. Xing, N.N. Guo, Y.T. Zhang, H.Q. Zhang, J.D. Liu, A negatively charged loose nanofiltration membrane by blending with poly (sodium 4-styrene sulfonate) grafted SiO2 via SI-ATRP for dye purification, Sep. Purif. Technol., 146 (2015) 50-59.

[40] J. Zhu, L. Qin, A. Uliana, J. Hou, J. Wang, Y. Zhang, X. Li, S. Yuan, J. Li, M. Tian, J. Lin, B. Van der Bruggen, Elevated Performance of Thin Film Nanocomposite Membranes Enabled by Modified Hydrophilic MOFs for Nanofiltration, ACS Applied Materials & Interfaces, 9 (2017) 1975-1986.

[41] H.C. Yang, J.Q. Luo, Y. Lv, P. Shen, Z.K. Xu, Surface engineering of polymer membranes via mussel-inspired chemistry, J. Membr. Sci., 483 (2015) 42-59.

[42] Q. Ye, F. Zhou, W.M. Liu, Bioinspired catecholic chemistry for surface modification, Chem. Soc. Rev., 40 (2011) 4244-4258.

[43] M.N. Abu Seman, M. Khayet, N. Hilal, Nanofiltration thin-film composite polyester polyethersulfone-based membranes prepared by interfacial polymerization, J. Membr. Sci., 348 (2010) 109-116.

[44] P. Silva, S.J. Han, A.G. Livingston, Solvent transport in organic solvent nanofiltration membranes, J. Membr. Sci., 262 (2005) 49-59.

[45] D. Bhanushali, S. Kloos, C. Kurth, D. Bhattacharyya, Performance of solvent-resistant membranes for non-aqueous systems: solvent permeation results and modeling, J. Membr. Sci., 189 (2001) 1-21.

[46] X.F. Li, S. De Feyter, I.F.J. Vankelecom, Poly(sulfone)/sulfonated poly(ether ether ketone) blend membranes: Morphology study and application in the filtration of alcohol based feeds, J. Membr. Sci., 324 (2008) 67-75.

[47] S. Sorribas, P. Gorgojo, C. Tellez, J. Coronas, A.G. Livingston, High Flux Thin Film Nanocomposite Membranes Based on Metal-Organic Frameworks for Organic Solvent Nanofiltration, J. Am. Chem. Soc., 135 (2013) 15201-15208.

[48] H. Zhang, H. Mao, J. Wang, R. Ding, Z. Du, J. Liu, S. Cao, Mineralization-inspired preparation of composite membranes with polyethyleneimine–nanoparticle hybrid active layer for solvent resistant nanofiltration, Journal of Membrane Science, 470 (2014) 70-79.

[49] S. Roy, S.A. Ntim, S. Mitra, K.K. Sirkar, Facile fabrication of superior nanofiltration membranes from interfacially polymerized CNT-polymer composites, Journal of Membrane Science, 375 (2011) 81-87.

[50] A.V. Volkov, V.V. Parashchuk, D.F. Stamatialis, V.S. Khotimsky, V.V. Volkov, M. Wessling, High permeable PTMSP/PAN composite membranes for solvent nanofiltration, Journal of Membrane Science, 333 (2009) 88-93.

[51] J.K. Holt, H.G. Park, Y. Wang, M. Stadermann, A.B. Artyukhin, C.P. Grigoropoulos, A. Noy, O. Bakajin, Fast Mass Transport Through Sub-2-Nanometer Carbon Nanotubes, Science, 312 (2006) 1034.

Highlights

1. A facile and fast interfacial design strategy is presented for the preparation of high structure-stable nanocomposite membranes.
2. Two problems are solved simultaneously – low structure stability of nanocomposite membranes and poor compatibility between an inorganic filler and a polymer matrix.
3. The fabricated membranes have great potential for SRNF.